RESEARCH ON MAPPING LEVEE LINES USING LIDAR DATA IN THE NAKDONG RIVER BASINS, SOUTH KOREA

Yunjae Choung[1]
[1]Department of Civil, Environmental and Geodetic Engineering, The Ohio State University, 470 Hitchcock Hall, 2070 Neil Avenue, Columbus, OH 43210, USA.
Email: choung.12@buckeyemail.osu.edu

KEY WORDS: Levee lines, LiDAR, Slope map, Smoothing spline

ABSTRACT: Mapping levee lines is important for describing the levee shapes and identifying erosions occurring on the levee surfaces. This research proposes a procedure for mapping levee lines using the airborne topographic LiDAR data. The procedure for mapping the levee lines using the LiDAR data is operated as follows: First, the DSM (Digital Surface Models) is generated from the LiDAR point clouds by using the linear interpolation and the median filtering. Then, the slope map is generated from the DSM by calculating the maximum rates of elevation difference between each pixel of the DSM and its neighboring pixels. The levee crown plates and the levee slope plates are separately generated from the slope map by the slope difference analysis. The levee slope plates are used to identify the locations of the levees in Nadong River Basins. The levee crown plates are used to extract the levee lines from the LiDAR data. The modified convex hull algorithm is employed to extract the points that are located along the boundary of the generated crown plate. Finally, the smoothing spline function is applied to construct the levee lines using the extracted boundary points.

1. INTRODUCTION

A levee is defined as "a man-made structure; usually an earthen embankment, designed and constructed in accordance with sound engineering practices to contain, control or divert the flow of water to provide protection from temporary flooding" (FEMA (Federal Emergency Management Agency), 2014). The elements that constitute a typical levee are illustrated in Figure 1.

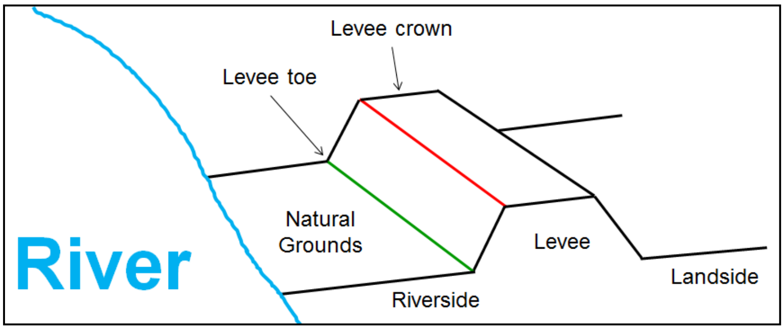

Figure 1. Elements of a typical levee (FEMA, 2014).

As seen in Figure 1, the levee crown is defined as "the flat surface at the top of a levee that is equal to or narrower than the base", and the levee toe is defined as "the edge of the levee where the base meets the natural ground" (FEMA, 2014).

The levee top line is defined as the line located between the levee's crown and slope plates (the red line in Figure 1), and the levee toe line is defined as the line between the levee slope plates and the natural grounds (the green line in Figure 1). In this research, both lines are defined as levee lines.

Levee line locations are generally determined by considering the surroundings, the geometric patterns, and the major objects on the levee surfaces. Historically, the levee lines are designed to be located on levee surfaces where the geometric patterns significantly change (MOLIT (Ministry of Land, Infrastructure and Transport), 2009). To protect the levee surfaces, the levee lines are located on the areas where the geometric patterns and the major materials are preserved (Kim *et al.*, 2004; Lee, 2010).

The utilization of the airborne topographic LiDAR (Light Detection and Ranging) data is efficient for mapping the coastal features such as the shorelines due to its ability to survey large areas rapidly and accurately (Liu *et al.*, 2009). Research on mapping the various coastal features has been carried out using the LiDAR data. Brügelmann (2000) developed a method for the extraction of the breaklines from the LiDAR data, taken in the coastal zones, using the grayscale images, which represent the range of the height component (*Z* coordinate) of LiDAR data. Briese (2004) proposed a method for extracting the coastal features from the LiDAR data using three-dimensional breakline models. Brzank *et al.* (2008) extracted the structure lines in coastal areas from the LiDAR data, using the tangent function. Choung *et al.* (2013) develops a method for extracting the coastal blufflines from the LiDAR data, using the breakline detection method.

This research aims at generating the levee lines from the LiDAR data taken in the Nakdong River Basins using the procedure explained in the following section.

2. METHODOLOGY

To represent the topographic surfaces using the grid format consisting of the constant cells, DSM (Digital Surface Model) is generated from the given LiDAR point cloud. The interpolation method is employed to estimate the elevation of each cell in the generated DSM. In general, slopes are significantly changed at the levee crown and toe surfaces. Hence, to detect the levee crown and slope plates, the linear interpolation method is used to generate the DSM because it has characteristics that describe the features, sharp edges, and steep surfaces (ArcGIS 9.2 Desktop Help, 2014). In general, DSM often includes outliers, which are the pixels that are significantly different in elevation compared with all the nearby pixels. These outliers are caused by random errors or objects such as utility poles, and these outliers, located near the levees, can cause difficulty when trying to detect levee mounds, which generally have gradual slopes. To remove these nearby outliers and to preserve the mounds that make up the levee's crown and slope plates, filtering is employed. In such research, a median filter is employed, which is a non-linear filter based on neighborhood ranking (Schenk, 1999; Wolf and Dewitt, 2000). The major advantages of median filtering over other linear filters are eliminating points with much larger values than the immediate neighboring points, and avoiding data modification (Liu *et al*., 2009; Schenk, 1999). The next step is to generate the slope map from the refined LiDAR DSM by calculating the maximum rates of elevation difference between each pixel of the refined LiDAR DSM and its neighboring pixels (ArcGIS 9.2 Desktop Help, 2014). In the generated slope map, an intensity value for each pixel represents the slope degree of the area. In general, the pixels with low slope values represent the objects that have relatively flat terrains, and the pixels with high slope values represent the objects that have relatively steep terrains. Figure 2 shows one section of the generated slope map.

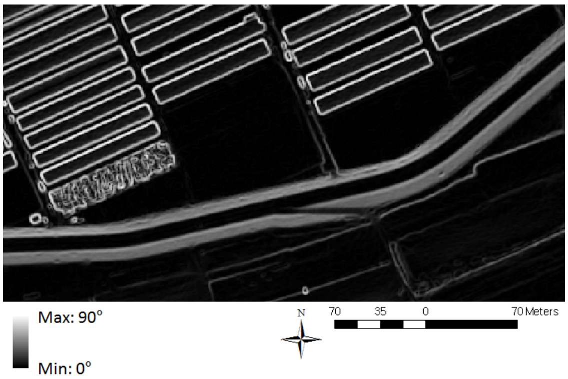

Figure 2. One section of the generated slope map.

Typical levees consist of steep plates with elevations that gradually increase from the toe to the crown on their surfaces, and flat plates with stable surface elevations. Steep and flat plates are separately generated from the slope map using the slope and elevation difference analysis. Historically, the levees constructed in South Korea are designed to have slope degrees from 18.43° (1V (Vertical):3H (Horizontal)) to 33.69° (1V:1.5H) on their slope plates (Lee, 2010; MOLIT, 2009). Considering the geometric changes, such as the erosions occurring on the levee slope plates, +/- 10° is added to the slope degree range for selecting the pixels representing the levee slope plates. Hence, the slope degree range for generating steep plates, including the levee slope plates, is set as [8.43°, 43.69°]. The slope degree range for the extraction of flat plates, including the levee crown plates, is set to avoid the first range and uses the lower degree values. Hence, it is set as [0º, 8.43º]. Using the above two ranges, the two types of plates (flat and steep plates) are separately generated from the slope map. In general, the steep plates represent the objects that have steep terrains, such as the levee slope plates, and the building walls, while the flat plates represent the objects that have flat terrains, such as the natural ground, the levee crown plates, highways, and roofs. Among the generated steep plates, the slope plate pairs located along a river course are selected to identify the levee locations. Then, among the flat plates located between the selected slope plate pairs, the plate with the highest elevation is selected as the levee crown plate, while the other flat plates are defined as the grounds, etc. The high resolution orthoimage showing the multiple levee components is shown in Figure 3(a), and the identified plates separately generated from the slope map are shown in Figure 3(b).

(a) High resolution orthoimage showing the multiple levee components.

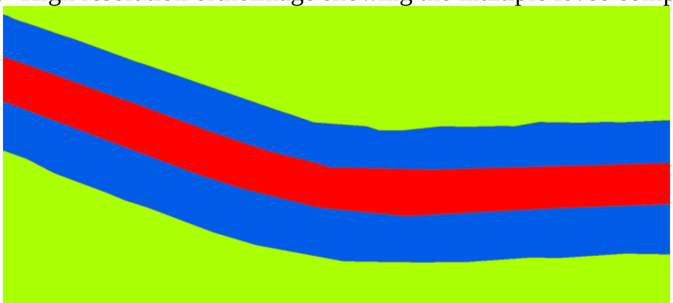

(b) Identified levee crown plate (a red polygon), the levee slope plate pairs (blue polygons) and the ground plates (green polygons).

Figure 3. The high resolution orthoimage showing the multiple levee components and the identified plates separately generated from the slope map.

The next step is to extract the levee lines using the LiDAR point groups located in the levee crown and slope plates. The levee lines of the levees constructed in South Korea are designed to have smooth-curve patterns (Lee, 2010). Hence, levee lines with smooth-curve patterns are created through the following steps. First, the boundary points of both the crown and slope plates are extracted from the LiDAR points using the modified convex hull algorithm. The modified convex hull algorithm procedure differs from the convex hull algorithm procedure because the latter generates the boundary for surrounding all the points, while the modified convex hull algorithm generates the boundary that comes into close contact with this point cloud's boundary point (Sampath *et al.*, 2007; Lee, 2012). Figure 4 shows an example of the boundary points (red dots) selected by the modified convex hull algorithm.

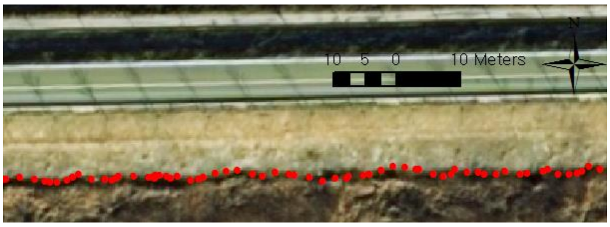

Figure 4. Example of the boundary points selected by the modified convex hull algorithm.

Second, the smoothing spline is used to create the levee lines with smooth-curve patterns, and to reduce the zigzag patterns caused by the noisy points included in the boundary. The smoothing spline uses the spline function by choosing the appropriate smoothing parameter (Mathworks, 2013). The smoothing spline s minimizes the residual sum of squares using the following equation (Mathworks, 2013):

$$p(\sum_i (y_i - s(x_i))^2) + (1 - p) \int s''(x)^2 dx \quad (1)$$

where p is a smoothing parameter, $s(x)$ is the smoothing spline function, and (x_i, y_i) is a sequence of observations. The value of p is defined as between 0 and 1, and $p = 0$ generally produces a linear polynomial fit to the data, while $p = 1$ generally produces a natural cubic polynomial fit that passes through all the data points (Mathworks, 2013). Hence, the curves generated by using smoothing parameters with high values have relatively sharp-curve patterns, while the curves generated by using smoothing parameters with low values have relatively smooth-curve patterns close to the straight line. To generate lines with smooth-curve patterns, low values are chosen for p based on an empirical analysis. Figure 5 shows the comparison of the levee lines (green or red lines) generated by the smoothing spline function using different p values with the reference lines (yellow lines).

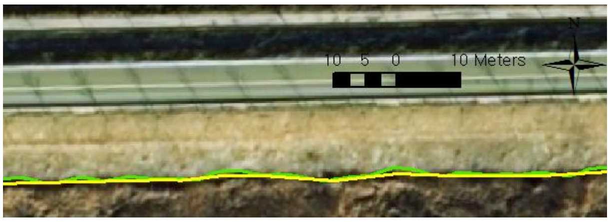

(a) Levee lines (green line) generated by setting the *p* value at 0.5 and the reference line (yellow line).

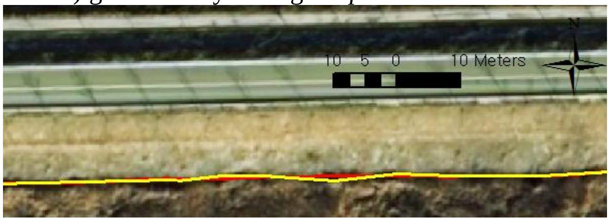

(b) Levee line (red line) generated by setting the *p* value at 0.1 and the reference line (yellow line).

Figure 5. Comparison of the levee lines generated by the smoothing spline function using the different *p* values and the reference lines.

Figure 5 shows that the levee lines generated by choosing the 0.5 and 0.1 smoothing parameters have smooth-curve patterns. The levee lines generated by choosing the 0.5 smoothing parameter, however, generate relatively sharp-curve patterns due to the noisy boundary points, while the levee lines generated by the 0.1 smoothing parameter have relatively smooth-curve patterns and are closer to the reference lines. Hence, 0.1 is chosen as the smoothing parameter in this study to create levee lines with smooth-curve patterns from the boundary point sets using the smoothing spline function. Finally, the levee top and toe lines are constructed through the above procedure.

3. STUDY AREA AND DATASET

The study area for this research is a river basin in a 22 kilometer stretch of Nakdong River, which passes through the South Korean cities of Changnyeong, Milyang and Changwon. This area is chosen for the following reasons. First, the availability of multiple remote sensing data sets such as the LiDAR data and the multispectral aerial orthoimages taken at about the same time, makes this region an excellent visual site for levee mapping tasks. Second, this region suffers serious damage caused by annual flooding events (WAMIS (WAter Management Information System), 2014). The LiDAR data was acquired in December 2009 using the ALTM Gemini 167 sensor at a speed of 234 kilometers per hour. The horizontal datum is International Geodetic Reference System (GRS) 1980, and the vertical datum is the mean sea level (MSL) at Incheon Bay, the vertical datum of Korean geodetic datum. The average point density of the given LiDAR data is 1.5 points / m^2. The horizontal accuracy is 15 cm and the vertical accuracy is 5 cm.

4. CONCLUSIONS AND FUTURE WORKS

This paper proposes a robust method for generating levee lines using the LiDAR data taken in the Nakdong River Basins. Multiple methods such as the smoothing spline and the slope difference analysis are employed to extract the levee lines. The works to be performed in the future work is to assess the accuracy of the generated levee lines.

Acknowledgement

The author would like to thank Dr. Rongxing Li for his academic assistance.

References

ArcGIS 9.2 Desktop Help, 2014. TIN to Raster (3D Analyst). Retrieved May 5, 2014, from http://webhelp.esri.com/arcgisdesktop/9.2/index.cfm?TopicName=TIN_to_Raster_%283D_Analyst%29.

ArcGIS 9.2 Desktop Help, 2014. Calculating slope. Retrieved May 5, 2014, from http://webhelp.esri.com/arcgisdesktop/9.2/index.cfm?TopicName=Calculating_slope.

Briese, C., 2004. Three-dimensional Modelling of Breaklines from Airborne Laser Scanner Data. Proceeding of the 10th.ISPRS Congress, July 12 - 23, Istanbul, Turkey, 35, B3, unpaginated CD-ROM.

Brügelmann, R., 2000. Automatic breakline detection from airborne laser range data. International Archives of Photogrammetry and Remote Sensing, 33(B3), pp.109-115.

Brzank, A., C. Heike, J. Goepfert, and U. Woergel, 2008. Aspects of generating precise digital terrain models in the Wadden Sea from lidar-water classification and structure line extraction. ISPRS Journal of Photogrammetry & Remote Sensing, 63(2008), pp. 510-528.

Choung, Y.J., R. Li, and M.H. JO, 2013. Development of a vector-based method for coastal bluffline mapping using LiDAR data and a comparison study in the area of Lake Erie. Marine Geodesy, 36(3), pp. 285-302.

FEMA, 2014. FEMA Levee Resources and Library. Retrieved May 5, 2014, from http://www.fema.gov/living-levees-its-shared-responsibility/fema-levee-resources-library.

Kim, K.H., D.K. Im, and H.K. Yeo, 2004. Inspection of the river basin for management of their natures. *Journal of* KWRA (Korean Water Resources Association), 37(4), pp.109-118.
Lee, I.C., 2012, Instantaneous Shoreline Extraction Utilizing Integrated Spectrum and Shadow Analysis from LiDAR and High-resolution Satellite Imagery. Ph.D. Dissertation, The Ohio State University, Columbus, OH, USA.
Lee, J.S., 2010, River Engineering and Design; Saeron Books. Seoul, S.Korea, 600 p.
Liu, J.K., R. Li, S. Deshpande, X. Niu, and T.Y. Shih, 2009. Estimation of Blufflines using Topographic LiDAR Data and Orthoimages, Photogrammetric Engineering and Remote Sensing, 75(1), pp. 69-79.
Mathworks, 2014. Smoothing splines, Retrieved May 5, 2014, from http://www.mathworks.com/help/curvefit/smoothing-splines.html.
MOLIT, 2009. Reports for management of Nakdong River basins in 2009, Retrieved May 5, 2014, from http://www.river.go.kr/WebForm/sub_04/sub_04_01_01.aspx.
Sampath, A., and J. Shan. 2007. Building boundary tracing and regularization from airborne LiDAR point clouds, Photogrammetric Engineering and Remote Sensing, 73(7), pp. 805-812.
Schenk, T., 1999. Digital photogrammetry: Volume I; Terra Science, Laurelville, OH, 428 p.
USACE, 2000. Design and Construction of Levees, Retrieved May 5, 2014, from http://www.publication.usace.army.mil/Portals/76/Publications/EngineerManuals/EM_1110-2-1913.pdf.
WAMIS, 2014. Estimated values damaged by annual flooding, Retrieved May 5, 2014, from http://www.wamis.go.kr/wrf/wrf_fddamaa_lst.aspx.
Wolf, P. R., and B.A. Dewitt, 2000. Elements of photogrammetry with applications in GIS, 3rd ed.; McGraw-Hill, New York, 688 p.